Mass concentrations of autumn bioaerosol in a mature temperate woodland Free Air Carbon Dioxide Enrichment (FACE) experiment: investigating the role of meteorology and carbon dioxide levels

Aileen B. Baird[1,2], Edward J. Bannister[1,2], A. Robert MacKenzie[1,2], and Francis D. Pope[1,2*]

5 [1]School of Geography, Earth & Environmental Sciences, University of Birmingham, Birmingham, B152TT, UK
[2]Birmingham Institute of Forest Research, University of Birmingham, Birmingham, B152TT, UK

Correspondence to: Francis Pope f.pope@bham.ac.uk

Abstract.

Forest environments contain a wide variety of airborne biological particles (bioaerosols), including pollen, fungal spores,
10 bacteria, viruses, plant detritus and soil particles. Forest bioaerosol plays a number of important roles related to plant and livestock health, human disease and allergenicity, forest and wider ecology, and are thought to influence biosphere/atmosphere interactions via warm and cold cloud formation. Despite the importance of bioaerosols, there are few measurements of forest aerosol, and there is a lack of understanding of how climate change will affect forest bioaerosol in the future.

We installed low-cost optical particle counters (OPCs) to measure particles in the size range between 1 and 10 µm, where
15 bioaerosols will likely dominate the particle mass concentration, for a period of two months in Autumn 2018 at the Birmingham Institute of Forest Research (BIFoR) Free Air Carbon Dioxide Enrichment (FACE) facility. The BIFoR FACE facility fumigates three 700 m^2 areas of the forest with an additional 150 ppm CO_2 above ambient with minimal impacts on other potential environmental drivers such as temperature, humidity, and wind. This experimental set-up enabled us to investigate the effect of environmental variables, including elevated CO_2 (eCO_2), on bioaerosol concentrations, and to evaluate the
20 performance of the low-cost OPCs in a forested environment.

Operating the low-cost OPCs during Autumn 2018, we aimed to capture predominantly the fungal bioaerosol season. Across the experimental duration, the OPCs captured both temporal and spatial variation in bioaerosol concentrations. Aerosol concentrations were affected by changing temperatures and wind speeds, but, contrary to our initial hypothesis, not by relative humidity. We detected no effect of the eCO_2 treatment on total bioaerosol concentrations, but a potential suppression of high
25 concentration bioaerosol events was detected under eCO_2. In-canopy atmospheric dispersion modelling indicates that the median spore dispersion distance is sufficiently small that there is little mixing between treatment and control experiments. Our data demonstrate the suitability of low-cost OPCs, interpreted with due caution, for use in forests, and so opens the possibility of forest bioaerosol monitoring in a wider range of habitats, to a wider range of researchers at a modest cost.

1 Introduction

30 Aerobiology investigates the production, transport, and removal of airborne biological particles such as bacterial, fungal, and viral microbes, plant pollen, and soil and plant debris. Fungal spores form a large proportion of the bioaerosol population, with ground level concentrations typically 10,000–50,000 spores m^{-3} (compared with 1000–2000 pollen grains m^{-3}) (Sesartic and Dallafior, 2011, and references therein). Modelling suggests that fungal spores form approximately 23% of bioaerosol mass globally (Heald and Spracklen (2009). Understanding the dispersal of fungal spores is not only essential for understanding

35 fungal ecology and their direct relevance to the forest plant and soil communities, but also for understanding human disease and allergens, plant and crop health, livestock health, as well as the role played by bioaerosols in ice nucleation and cloud condensation (Pöschl, 2005; Reinmuth-Selzle et al., 2017; Sesartic and Dallafior, 2011). The significant influence of airborne fungal particles on forest biology is often overlooked.

Spores are produced by fungi as propagules during asexual and sexual reproduction (Læssøe and Petersen, 2019). Fungal

40 spores are varied in shape and size, with typical diameters of 1–30 µm, although their diameters can vary from 1–1000 µm (Fröhlich-Nowoisky et al., 2009; Halbwachs and Bässler, 2015; Jones and Harrison, 2004). Spore dispersal is a complex process, affected by size and shape of the spores, meteorological and ecological factors, and the life history of the fungus. Fungi which produce below-ground fruit bodies, and some mycorrhizal fungi without sporocarps, rarely have spores in significant concentrations in the air, and are more commonly spread by animals. Above-ground fungal fruiting bodies with

45 active release mechanisms or tall stipes may release spores higher into the air (Biedermann and Vega, 2020; Dressaire et al., 2016; Halbwachs and Bässler, 2015; Horton, 2017; Kivlin et al., 2014; Lilleskov and Bruns, 2005; Stephens and Rowe, 2020). Spore size, shape, and ornamentation influence their dispersal, with smaller and/or less dense spores able to travel further, although even very large spores may be dispersed by the air (Chaudhary et al., 2020; Norros et al., 2014, 2012). In addition to the spore and fungal characteristics, the meteorology and ecology of the environment both significantly influence spore

50 dispersal (Halbwachs and Bässler, 2015; Oneto et al., 2020). Mature forests generally have complex, multi-layered canopies which affect airflow through the forest, in addition to altering temperature and relative humidity (RH) variability (Bannister et al., 2021; Gilbert and Reynolds, 2005; Norros et al., 2014).

Meteorological factors have also been shown to impact airborne fungal communities significantly. Several studies have measured concentrations of airborne fungal spores in UK (largely in cities), investigating diurnal and seasonal variables as

55 well as meteorological variables on fungal spores. The effects are almost always species-specific, with a broader seasonal trend of fungal spore concentrations being highest in late summer and autumn (Hollins et al., 2004; O'Connor et al., 2014; Sadyś et al., 2016a, 2014). Larger European studies (e.g. Grinn-Gofroń et al., 2019) and reviews have shown that the two most influential meteorological variables for airborne fungal spore concentrations are temperature and RH (Jones and Harrison, 2004; Moore-Landecker, 2011).

60 As well as being affected on shorter time scales by meteorological factors, airborne fungal concentrations can also be affected by climate change, both due to increases in CO_2 concentrations as well as the corresponding increase in temperature, although

effects on fungi may vary depending on the species (Burge, 2002). Wolf et al. (2003) tested the response of 11 arbuscular mycorrhizal (AM) fungi to eCO_2 at the BioCON FACE grassland experiment, with only a single *Glomus* species producing additional spores in the soil. Wolf et al. (2010) demonstrated an increase in spore production from *Alternaria alternata* (a

65   common airborne allergen) under eCO_2 in a growth chamber. Similarly, in an Aspen tree (*Populus tremuloides*) open-topped chamber eCO_2 experiment, Klironomos et al. (1997) found that airborne fungal spore concentrations increased, which they suggested was due to corresponding increases in spore concentrations in the leaf litter.

In addition to direct changes in spore production, it is possible that fungal sporocarp production, and therefore spore production, could also increase due to climate change. Ecological measurements show the autumn fungal fruiting seasons in Europe have

70   become longer over the last 50 years. The fungal fruiting season starts earlier and finishes later due to climate change, in addition to more fungi having an additional spring fruiting season (Gange et al., 2007; Kauserud et al., 2012). This climate-induced phenology change has also been demonstrated in a corresponding increase in the airborne fungal spore season (Sadyś et al., 2016b). These large changes in the fungal season were mainly attributed to temperature increases; however, at the Aspen FACE experiment, it was found that ectomycorrhizal fungi sporocarp production increased under eCO_2, so it seems possible

75   that CO_2 impacts fungal sporocarp production independently of temperature (Andrew and Lilleskov, 2009).

The studies described above demonstrate that fungi are likely to change spore and sporocarp production under eCO_2 ranging from 192–600 ppm, in addition to the significant changes witnessed in fungal growing seasons under the current anthropogenic increases and broader climate effects. Even if these findings are fungal species-specific, they indicate that fungal bioaerosols concentrations can be expected to change under eCO_2, with potentially wide-ranging effects for forested habitats (Baird and

80   Pope, 2021) . However, none of the above studies were completed in complex mature woodlands, with the experiments being completed in laboratories, open-topped chambers or, in the case of Aspen FACE, a young plantation forest. Mature and ancient woodlands represent a more complex and diverse environment, which are likely to respond differently to eCO_2 than the plantations of young trees on agricultural soil studied in earlier FACE experiments (Norby et al., 2016). There are also few studies of forest airborne spore concentration responses to eCO_2, with the majority of studies focussing on sporocarp

85   production.

In order to study airborne forest fungal bioaerosols under eCO_2 in a mature temperate woodland, we installed low-cost Optical Particle Counters (OPCs) into the BIFoR FACE experiment during Autumn 2018.

Our hypotheses were:

   A) Hourly fungal bioaerosol concentrations will correlate with hourly weather conditions (wind, RH, temperature).

90   B) Fungal bioaerosol concentrations will increase in woodland patches treated with eCO_2 for two years.

2 Methods

2.1 BIFoR FACE

The BIFoR FACE experiment is located in a 19.1 hectare mature oak forest in Staffordshire. The overall aim of the FACE experiment is to mimic the effects of anthropogenic climate change by increasing the CO_2 concentrations in areas of the forest

95 by 150 ppm above ambient (~400 ppm) (MacKenzie et al., 2020; Norby et al., 2016). This set-up is one of only two FACE experiments in mature forests worldwide and it provides a unique experiment to study mature temperate woodland. In the context of bioaerosols, this experiment allows the investigation of the direct and indirect effects of eCO_2 in a minimally disturbed forest environment (Hart et al., 2019).

As shown in the site map in Figure 1, the CO_2 enrichment set-up consists of nine roughly circular "arrays" of three types, each

100 array being approximately 30 m in diameter. Arrays 1, 4, and 6 are fumigated with additional CO_2, increasing the atmospheric CO_2 by 150 ppm above ambient (to approximately 550 ppm). The CO_2, pre-mixed with air, is released into the tree canopies, using pipes running the height of 25 m tall towers around the perimeter of the array. Arrays 2, 3, and 5 have the same tower set-up, but fumigate only with air. Arrays 7, 8 and 9 are "ghost" arrays without any fumigation infrastructure. Arrays 1–6 are grouped into three treatment pairs, based on pre-fumigation vegetation and soil biochemistry analysis, each with a single

105 elevated CO_2 and single ambient CO_2 array. The array pairs are as follows: 1 and 3; 2 and 4; 5 and 6. The present study used Arrays 1–6 only, measuring in each pair of arrays consecutively. Fumigation occurs during the oak growing season, approximately 1st April to 31st October during daylight hours. In 2018, CO_2 fumigation ended on the 31st October 2018 at sundown.

The predominant tree species in the woodland is *Quercus robur* (English oak), with *Corylus avellana* (Hazel) forming a distinct

110 understory layer. Other tree species present include *Acer pseudoplanatus* (Sycamore), *Crataegus monogyna* (Common Hawthorn), and *Ilex spp.* (Holly). A recent vegetation survey, in 2019, was completed to determine the major ground plant species: *Rubus fruticosus* (Bramble)*, Phegopteris connectilis* (Beech fern), a *Hedera sp.* (Ivy), and grasses where the canopy has been opened for access rides (G. Platt, private communication, 2019). Hanging and fallen deadwood is left in place except where it poses a direct health-and-safety risk.

115 In order to focus on the fungal bioaerosol component, we took measurements during the autumn, when pollen and non-fungal spore counts from the dominant vegetation were likely to be low. For example, the pollen counts are highest in spring for the two dominant tree species at BIFoR FACE. UK oak pollen season can range from March to July and lasts for 4–8 weeks, with peak concentrations usually occurring in May (Grundström et al., 2019). Hazel pollen season falls earlier in the year, starting as early as January, peaking in February or March (National Pollen and Aerobiology Research Unit, 2012). For ground cover

120 species, the grass pollen season peaks in the summer months, sometimes extending into early September (National Pollen and Aerobiology Research Unit, 2012), and *P. connectilis* sporulation peaking mid-July until mid-September (Page, 1997). None of these pollen and fern sporulation seasons coincide with our measurement period. Our measurement period coincides with

the fungal fruiting season at BIFoR (see below), as well as previously measured peaks in UK fungal spore concentrations (Davies et al., 1963).

125 Monthly macro-fungi surveys were completed during the OPC measurement period. These surveys revealed the annual peak of fungal fruiting in 2018 occurred across September and October at BIFoR FACE. Species fruiting in October 2018 included, but were not limited to: *Lactarius quietus* (oakbug milkcap), at least one *Russula* (Brittlegill) species, *Lycoperdon perlatum* (Common puffball), *Mycena rosea* (Rosy Bonnet) and other *Mycena* species, *Auricularia auricula* (Jelly ear), *Hypholoma fasciculare* (Sulphur tuft), *Xylaria hypoxylon* (Candlesnuff Fungus), and a number of resupinate fungi, including several

130 *Stereum* species. All of these fungi produce spores in the range of 3–9 µm, matching the measurement capabilities of the OPCs (Læssøe and Petersen, 2019). *Auricularia auricula* is an exception; it was observed but produces larger, 16–18 µm-long spores likely outside the OPC size window.
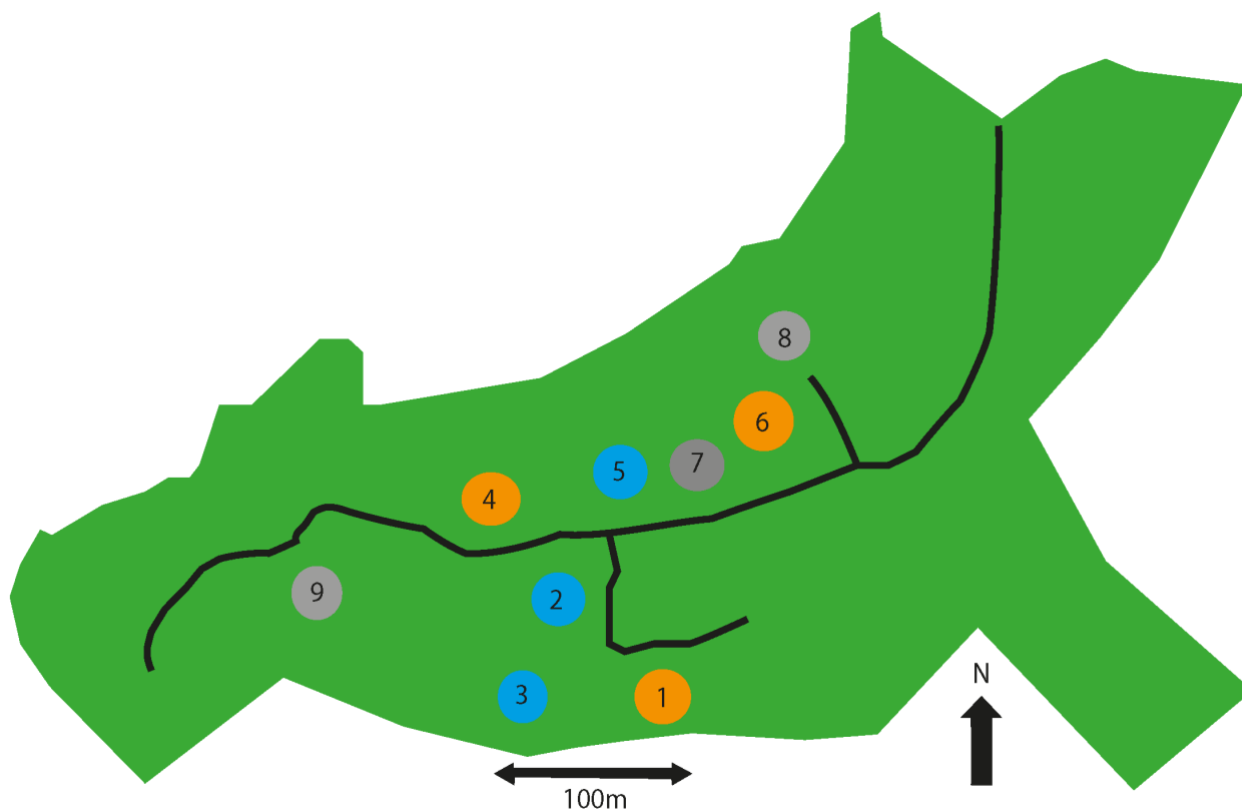
Figure 1. Map of the BIFoR forest and FACE facility located in Staffordshire (UK) adapted from Hart et al., 2019. The green area
135 **shows the whole 19.1 ha Mill Haft woodland, 7.3 ha of which is controlled by the University of Birmingham. The access road is shown as a thick black line. Circles represent scientific research "arrays". Orange arrays 1, 4, and 6 are surrounded with 25 m tall towers. CO_2 levels inside the array are raised by fumigation to 150 ppm above ambient (from ~400 ppm to ~550ppm). Blue arrays**

Biogeosciences
Discussions

Open Access

EGU

140   **2, 3, and 5 have similar towers, but are an infrastructure control, spraying out air with current ambient concentrations of CO₂. Grey arrays 7, 8, and 9, are non-infrastructure controls, with no towers or fumigation. Treatment and control arrays 1–6 are paired as follows: 1 and 3, 2 and 4, 5 and 6. The landscape surrounding BIFoR FACE is predominantly young tree plantations of mixed broadleaves and conifers (MacKenzie et al., 2020).**

2.2 Instrumentation

In this study, we use optical particle counters, OPC-N2 sensors (Alphasense, Essex), which count and size particles between 0.3 µm and 10 µm in diameter. The sensors are described in detail by Crilley et al. (2018) and Sousan et al. (2016). In brief,

145   the OPCs count the number of particles, and use particle light scattering to determine particle size using Mie scattering approximations. To calculate particle mass concentration, particles are assumed to be of uniform spherical shape, the density is assumed to be 1.65 g cm^{-3} and the refractive index is assumed to be 1.5. It is noted that fungal spores, the target of this study, are often ellipsoidal in shape and can be defined by a short and long axis diameter. Different fungal species generate spores with different shapes and sizes. The assumptions used by the OPC are typically wrong on a single particle (or

150   bioaerosol) basis but should approach reality on an ensemble averaged basis.

The sensors do not explicitly discriminate between particle types, so in order to discriminate between fungi and other smaller particles (bacteria and anthropogenic aerosols), we excluded data from particles smaller than 1 µm in diameter, measuring from 1 µm up to the maximum 10 µm measuring capacity of the OPCs. This size discrimination, in conjunction with the experimental location and seasonal timing of the experiment make it highly likely the majority of bioaerosols being captured

155   are predominantly of fungal origin.

One of the key concerns raised for the sensing of any aerosol type using low-cost OPCs is that they can report artificially high readings under high RH conditions. Hygroscopic aerosols take up water from the surrounding gaseous environment as a function of RH, with greater water uptake at higher RH. To compare the abundance of aerosol under different environmental conditions, it is preferable to use a 'dry' aerosol concentration, with the hygroscopic growth due to water removed. To

160   parameterise particle hygroscopicity, κ-Köhler theory is used, which describes the particle hygroscopicity using a single hygroscopicity parameter kappa (κ) (Petters and Kreidenweis, 2007). Pope (2010) details how κ-Köhler theory can be used to link particle mass to hygroscopicity by Eq. (1).

$$a_w = \frac{\left(\frac{m}{m_0} - 1\right)}{\left(\frac{m}{m_0} - 1\right) + \frac{\rho_w \kappa}{\rho_p}} \tag{1}$$

a_w is equilibrium RH expressed as a decimal, m is the wet aerosol mass, m_0 is the dry aerosol mass, and ρ_w and ρ_p the density

165   of water and the dry particulate, respectively. The value of κ can be found by curve fitting of the pollen humidograms (m/m_0 versus a_w).

Biological particles such as fungal spores and pollen have been demonstrated to be hygroscopic, although they typically have a low kappa (κ) value, with pollen κ typically around 0.05–0.1 as opposed to a κ of approximately 0.3 for average anthropogenic aerosols (Griffiths et al., 2012; Pope, 2010). Due to the hygroscopicity of fungal aerosols, high relative humidity can result in

170 a high mass concentration reading in sensors, such as the low-cost OPCs, which do not warm or dry the air. This hygroscopic effect has been explored using low-cost OPCs in urban environments by Crilley et al. (2020, 2018), where they used a calibration factor to correct for RH effects.

2.3 Instrument installation, bias-checking, and calibration

We used a pair of low-cost OPCs to study bioaerosols at BIFoR FACE. The two OPCs used were controlled to take
175 measurements every 60 seconds using a Raspberry Pi computer (Crilley et al., 2018, based on Hagan, 2017). The OPCs and accompanying instrumentation were installed in a pair of BIFoR FACE arrays at a time (according to the pairing detailed in Section 2.1), between 9th November and 13th December 2018, as per **Error! Reference source not found.**. The air inlet for each Optical Particle Counter was orientated towards the south-west in order to face the predominant wind direction for the site (Hart et al., 2019).

180 Two Tinytag Plus 2 TGP-4500 (Gemini data loggers, Chichester, UK) units were used to measure RH and temperature alongside the low-cost OPCs. The units measure temperature from -25°C to +85°C using an internally mounted thermistor, with the manufacturers stating an accuracy of 0.01°C or better. Under field conditions, the TinyTag sensors closely follow temperature measurements taken by a weather station located at 2 m height in Array 1, with the mean temperature measured by the TinyTags measuring within 0.4°C of the weather station. RH is measured using an externally mounted capacitive sensor,
185 from 0–100% RH, with a manufacturer stated accuracy of +/- 3.0% RH at 25°C. Tinytag units were placed on the top of the OPCs, with the RH sensor facing in the same direction as the OPC inlet.

Above-canopy wind speed was measured using two-D ultrasonic anemometers (WMT700, Vaisala) ~1 m above the canopy (~25 m height) on the northernmost tower of array 1. Below-canopy wind speed and direction (~2 m height) were measured using 03002-L Wind Sentry set (Campbell Scientific, Loughborough, UK) located to the right of the metal walkway near the
190 entrance of Array 1. The manufacturer stated minimum threshold wind speed was 0.8 m s^{-1} for the Campbell anemometer, with 2 m height wind speeds below this minimum threshold considered as zero for the purposes of this experiment.

Table 1. Table listing the dates (dd.mm.yyyy) and locations of equipment installation across the experimental duration at BIFoR FACE. Both optical particle counters (OPCs) and TinyTag relative humidity and temperature sensors were installed simultaneously.

Date range	Tiny Tag unit	OPC unit	Array number	eCO$_2$ or Ambient
09.11.2018-	A	1	A2	Ambient
21.11.2018	B	2	A4	eCO$_2$
21.11.2018-	A	1	A6	eCO$_2$
30.11.2018	B	2	A5	Ambient
05.12.2018-	A	1	A1	eCO$_2$
13.12.2018	B	2	A3	Ambient

195

Both the pair of OPCs and TinyTags were installed for a six day side-by-side intercomparison period at 1.5 m height in Array 1 of BIFoR FACE from 30th November 2018 until 05th December 2018. Using the data from this intercomparison week, bias calibration factors were calculated.

200 No bias factor was applied to the temperature data from the TinyTag units. RH data from the TinyTags was first filtered to remove any measurements lower than 50% and greater than 99%, and a calibration bias factor of 1.03 applied to TinyTag Unit B to make the two units consistent with each other. A similar calibration was performed on the particulate matter (PM) data collected by the OPCs, with the data from OPC 1 being increased by a bias factor of 1.45. Bias factors were calculated from the six-day side-by-side period, with the factor applied to the data from the full measurement period of 37 days. This bias correction ensured the two OPCs were consistent with each other.

205 For both the TinyTag and OPC pairs, the consistency between the two instruments, rather than absolute calibration, was more important to allow for observation of differences between two different locations. Hence one instrument of each pair was bias-corrected to the other instrument of the pair. However, a comparison outside of the forest environment was completed between the low-cost OPCs and a TSI 3330 (a reference grade OPC), with the low-cost OPCs measuring within 25% of the TSI without any humidity corrections, which is considered a good performance for the low-cost sensors (Crilley et al., 2020, 2018).

210 **2.4 Spore dispersal model**

We developed a conceptual model to help interpret the OPC results from BIFoR FACE. Within dense forests, the mean horizontal wind speed U inflects around the tops of the trees, increasing approximately exponentially with height below the inflection and logarithmically with height above it (Bannister et al., 2021; Cionco, 1965; Finnigan, 2000; Raupach et al., 1996). Mean horizontal wind velocity U at each height z inside the canopy can, therefore, be approximated via Eq. (2):

215
$$U(z) = U_{h_c} e^{-a\left(1-\frac{z}{h_c}\right)} \tag{2}$$

where h_c is the mean height of the trees and U_{h_c} is U at h_c. The attenuation coefficient, a, accounts for the flow's response to the density of the forest and tends to increase with increasing leaf area index (LAI) and flexibility of the plant elements (Cionco, 1978; Kaimal and Finnigan, 1994) The exponential relationship in Eq. (2) does not hold in forests with a sparse trunk space and open edges, e.g. many pine plantations, for which a secondary wind velocity maximum occurs below the main crown

220 (Baldocchi and Meyers, 1988). However, it provides a reasonable first approximation for a forest such as that at the BIFoR FACE site, with extensive understorey growth and closed edges during the leaf-on season.

We adapt the model of Nathan et al., 2002 by using this exponential velocity profile to obtain a rough estimate of the horizontal distance over which spores disperse in a dense forest, D. We consider spores evenly distributed within small air parcels within the canopy airspace. D equals the distance an air parcel carrying spores travels between the time of release ($t_0 = 0$) and the

225 time at which the spores in the parcel settle on the ground (t_1). As a simplification, here we consider spore 'release' to include both detachment by the mean wind and the point at which spores begin to settle back to the ground after being swept upwards by short intense gusts (Aylor, 1978). For a spore falling at an average settling velocity v_s, $t_1 = h_r/v_s$, where h_r is the height

of spore release. The vertical position of spores within an air parcel during settling at time t is $z(t) = h_r - v_s t$. Substituting this expression into Eq. (2), we generate Eq. (3):

230

$$U(t) = U_{h_c} e^{-\frac{a}{h_c}(h_c - h_r + v_s t)} \tag{3}$$

The horizontal distance over which the spores disperse is therefore:

$$D = \int_0^{t_1} U(t) dt \tag{4a}$$

which, taking $t_1 = h_r / v_s$ and $U(t)$ from Eq. (3), gives:

$$D = \frac{U_{h_c} \cdot h_c}{a v_s} \left[e^{-a} \left(e^{\frac{a h_r}{h_c}} - 1 \right) \right] \tag{4b}$$

235 This model assumes the mean wind profile has already adjusted to the presence of the forest, for example, after passing into the forest from surrounding rural areas (see below).

We specified the mean height of the trees as 25 m to reflect those at the BIFoR FACE site. Reported values of a for forests fall within a relatively narrow range of around 1.5–4.8 (Amiro, 1990; Cionco, 1978; Su et al., 1998). We took $a = 2.5$, as measured for forests of similar LAI to BIFoR FACE (Su et al., 1998). Sensitivity testing (not shown) indicated that using higher and

240 lower values of a respectively decreased and increased the occurrence of spores travelling long distances, but had little effect on the modal value of D. i.e. using a lower a thickened the right tail of the probability density function of D but affected its peak relatively little.

We performed a stochastic ensemble of model runs ($n = 1,000,000$) in R (version 4.0.3, http://cran.r-project.org) with low (0–2 m s^{-1}), low-medium (*med-l*) (2–3 m s^{-1}), high-medium (*med-h*) (3–4 m s^{-1}), and high (4–6 m s^{-1}) mean wind speeds at the top

245 of the canopy, U_{h_c}. We considered only spores in the bottom 10 m of the forest airspace, i.e. h_r in the range 0–10 m. Strong turbulent fluxes of momentum, and scalar quantities such as spores, occur in the upper region of forest canopies (Belcher et al., 2012; Finnigan, 2000), which this simplified model cannot capture. Mean settling velocity, v_s, was specified in the range 0.001–0.005 m s^{-1}, taking reported values for fungal spores in the size range 1–10 µm (Di-Giovanni et al., 1995; Tesmer and Schnittler, 2007). For each model run, for we specified a random value of U_{h_c}, h_r and v_s from a uniform distribution within

250 each of these ranges (using the *runif* function in R).

3 Results

3.1 Hypothesis A: Hourly fungal bioaerosol concentrations will correlate with hourly weather conditions (wind, RH, temperature).

During the experimental period, there was a total of 46.3 mm of precipitation, with a median temperature of 7.7°C within the

255 forest. The lowest recorded temperature was -1.8°C, and the highest 15.8°C. The average daily temperature peak (and the lowest RH point) occurred at approximately 13:00 local time. RH was high throughout the measurement period, median and

Biogeosciences
Discussions

mean measured between 89–91% RH across the duration of the experiment, with the lowest recorded measurement at 63% RH. Wind speed patterns followed each other closely above and below the canopy, with below canopy measurements significantly lower. The mean wind speed above the canopy was 2.7 m s^{-1}, whereas below the canopy it was 0.4 m s^{-1}.

260 Figure 2 Panel A shows the relationship between RH and bioaerosol concentrations at BIFoR FACE: the curve is almost horizontal from 75–90% RH, where at 90% it rapidly increases, most likely indicating the particles becoming exponentially hygroscopic at very high humidities. This sudden increase in particle size at very high humidities demonstrates a clear hygroscopic effect; we therefore performed a correction factor to the data from Crilley et al., 2018, using a κ values of either 0.3 or 0.1 (Griffiths et al., 2012; Pope, 2010). Before correction, the median hourly PM_{10}–PM_1 concentration under eCO_2

265 conditions was 15.7 µg m^{-3} and 16.7 µg m^{-3} under ambient conditions (Figure 2 Panel A). After the application of the Crilley et al. correction factor using a κ of 0.3, this decreased to a median of 5.3 µg m^{-3} under eCO_2 and 5.9 µg m^{-3} at ambient CO_2 concentrations (Figure 2 Panel B), and using a κ of 0.1, the median was 9.3 µg m^{-3} under eCO_2, and 10.1 µg m^{-3} under ambient conditions (Figure 2 Panel C). The ratio between the mean concentrations obtained from the eCO_2 and ambient plots depend upon whether the Crilley correction factor is used and what value is used for κ. The values are 94%, 90%, and 92% for the

270 uncorrected ratio, the ratio using κ = 0.3 and the ratio using κ = 0.1, respectively. A comparison of the data before and after correction is shown in Figure 2 panels D, E, and F. Due to the decrease in PM concentrations, with respect to RH, shown using a κ of 0.3, the data corrected using a κ of 0.1 was used for all further analyses, as this was deemed more appropriate given the likely particle composition (low hygroscopicity bioaerosols). After correction to remove the instrument artefacts, there was no clear effect of RH on bioaerosol concentrations.
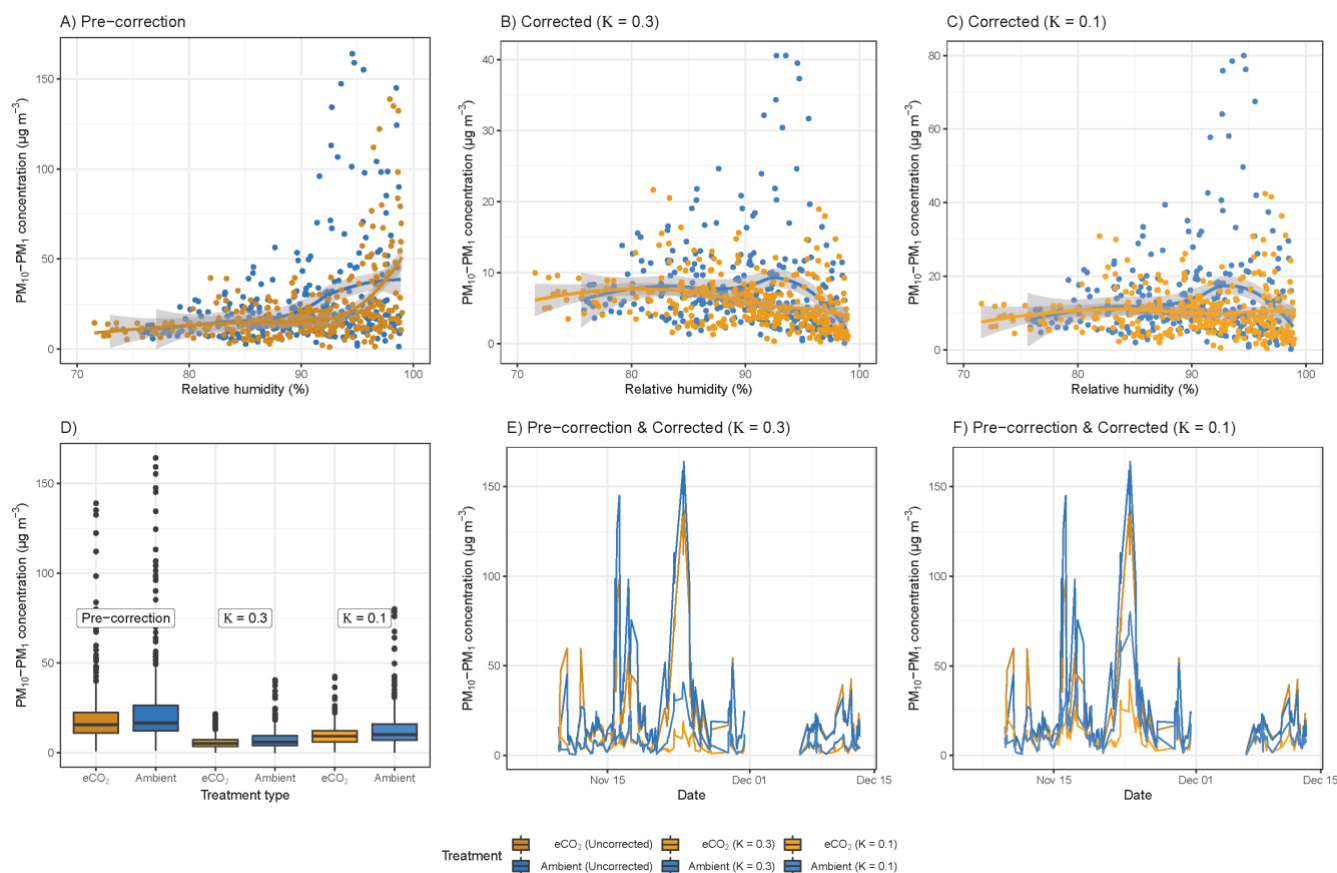
Figure 2. Relative humidity and bioaerosol concentrations (PM_{10}–PM_1) at BIFoR FACE in Autumn 2018. Panel A shows PM_{10}–PM_1 concentrations with increasing RH without any correction applied. Panels B and C plots the same data as Panel A, however a correction factor from Crilley et al., 2018 has been applied to the bioaerosols data to correct for the hygroscopic effect of the particles, Panel B using a κ of 0.3, and Panel C a κ of 0.1. Panels A, B, and C, all have loess curves fitted (Wickham et al., 2019). Panels D, E, and F compare the data before and after corrections. All the plots show PM_{10}–PM_1 concentrations under ambient conditions (Arrays 2, 3, and 5) in blue colours, and eCO_2 conditions (Arrays 1, 4, and 6) in orange colours, with the colour intensity varying depending on the correction factor applied.

The effects of wind speed and direction on the bioaerosol concentrations were also investigated in depth. Anemometers were located both above (25 m height) and below (2 m height) the canopy, with below-canopy measurements broadly following those above the canopy but measuring significantly lower at the lower height (Figure 3 Panel A). Above the canopy, the hourly wind speed never dropped below 0.8 m s^{-1}, whereas recorded speeds of 0 m s^{-1} (i.e. below anemometer threshold) were common below canopy. The maximum hourly wind speed above canopy was 7.05 m s^{-1}, compared with 2.59 m s^{-1} below canopy.

Bioaerosol concentrations demonstrated high variability under changing wind speeds; however, a possible U-shaped curve was observed, with higher bioaerosol concentrations at the lowest and highest wind speeds measured, as shown in Figure 3 Panels B and C. This effect was shown using the wind speeds taken from both above (25m) and below (2m) the canopy. Figure 4 shows the effect of wind speed and direction on bioaerosol concentrations using *openair* polar bivariate plots (Carslaw and

Ropkins, 2012). Observed wind speed patterns follow broadly similar trends between each pair of arrays, with the majority of medium concentration (medium concentration (green-yellow) bioaerosol activity occurring in the SW and SE quadrants, and only low (blue) concentrations under northerly winds. Peaks in bioaerosol concentration (presumed high sporulation events)

295   are visible in red, with some events being replicated across both eCO₂ treatment and control (e.g. the SW quadrant event in A5 and A6), and other events only occurring in a single array (e.g. the SE quadrant event in A4). Detecting events occurring in a single array at a time shows that the OPCs can detect differences between the BIFoR FACE arrays.

To investigate the relationship between spore dispersal and wind speed further, we used the model outlined in Section 2.4 to investigate the horizontal distance over which spores disperse, D. The model was run (n = 1,000,000) for spore release heights

300   (h_r) of 2 m, 5 m, and 10 m. Figure 5 shows the probability density functions of D under four wind speed scenarios: low, low-medium, medium-high, and high. As would be expected, generally, the lower the spore release height and wind speed, the shorter the overall distance travelled by spores. Most wind conditions experienced at BIFoR FACE fall under the "low" wind speed scenario (black lines), for which the modal distance travelled by spores were less than 20 m for all release heights (Figure 5). With the arrays having diameters of 25–30 m, this means that under typical conditions, we could expect spores to stay

305   within the array they were released in or, at least, very unlikely to be transported into neighbouring arrays (i.e. a spore released under eCO₂ is unlikely to be measurable in an ambient array in low wind conditions). However, at higher wind speeds, a heavy tail is present on each of the plots, indicating that spores are more likely to travel much greater distances at higher wind speeds, potentially causing mixing between the arrays. Finally, we looked at PM_{10}-PM_1 concentrations under changing temperature (Figure 6). There was a small linear positive relationship between temperature and bioaerosol concentrations, with PM_{10}-PM_1

310   concentrations of around 5 µg m^{-3} at the lowest temperatures (1-3 °C), increasing up to 10 µg m^{-3} at the highest temperatures of 12-13 °C.
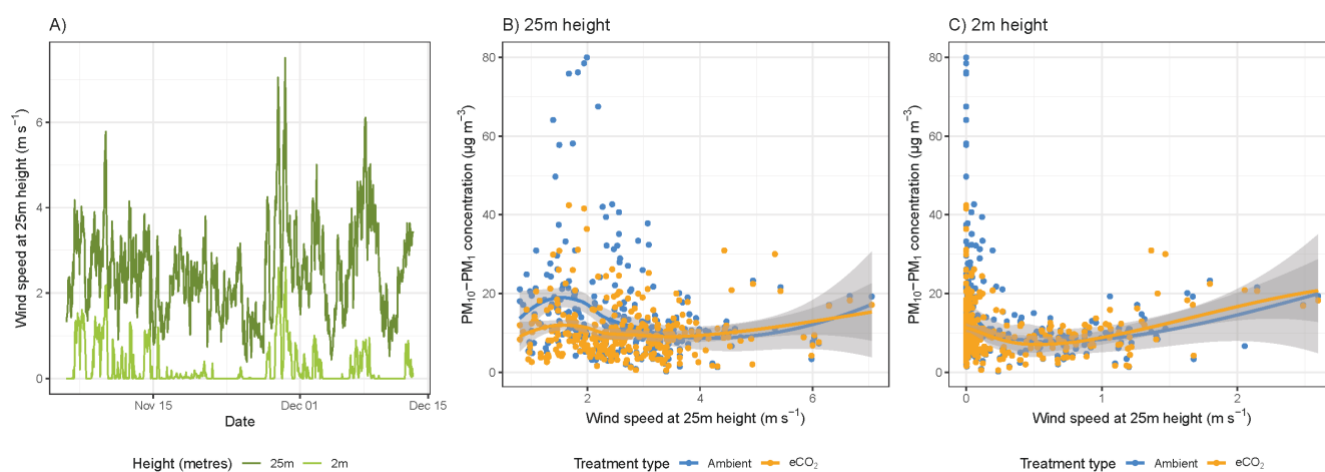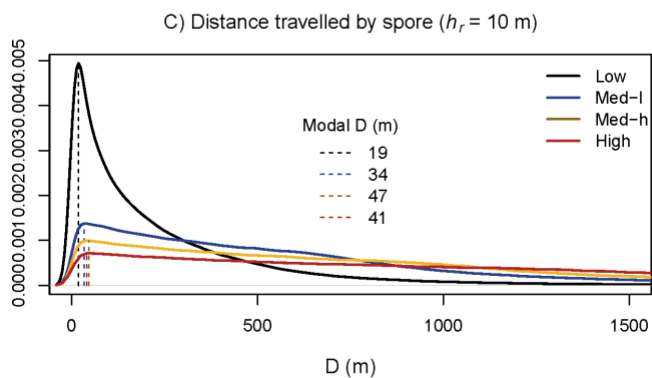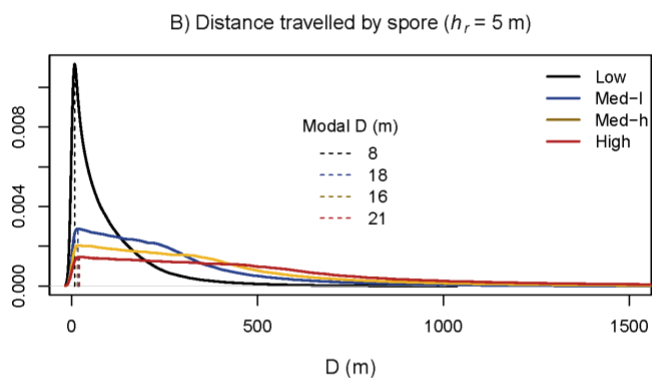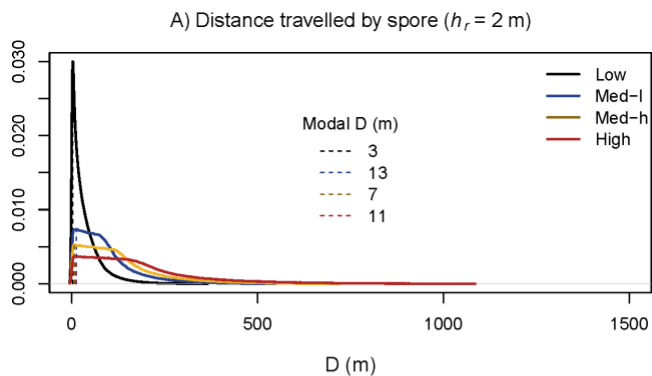

Figure 3. Wind speed and bioaerosol concentrations at BIFoR FACE in Autumn 2018. Panel A shows the wind speeds above (25 m height) and below (2 m height) the canopy across the experimental duration. Wind speed data at 25 m height is in dark green, and
315   **data from 2 m height in light green. Panels B compares hourly average PM_{10}–PM_1 concentrations with hourly average wind speeds measured at 25 m height, and Panel C the same PM_{10}–PM_1 concentrations using wind speeds measured at 2 m height. Panels B and**

C both have loess lines of fit (Wickham et al., 2019), with data from ambient arrays (Arrays 2, 3, and 5) in blue, and data from eCO_2 arrays (Arrays 1,4, and 6) in orange.
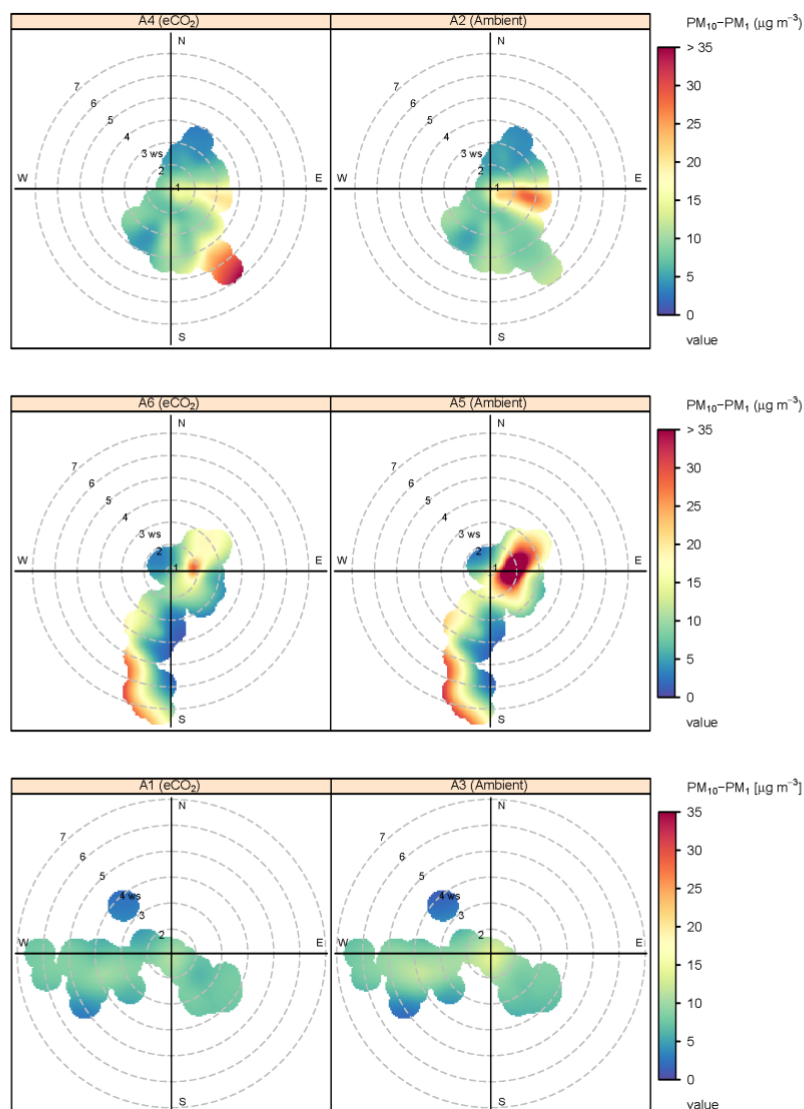

Figure 4. Openair polar bivariate plots showing bioaerosol concentrations (PM_{10}-PM_1) with wind speed and direction across the Autumn 2018 experimental duration at BIFoR FACE (Carslaw and Ropkins, 2012). Plots are displayed in the three array pairs (one eCO_2, one ambient) in which the pair of OPCs were located. Dates of OPC installation in each array pair are detailed in Error! Reference source not found.**. Bioaerosols were measuring using the OPCs at 2 m height, and wind data was taken from the anemometers at 25 m height. Colour gradients display the concentrations of bioaerosols detected, with low concentrations shown in blue/green colours, mid concentrations in yellow, and high concentrations in orange/red.**

A) Distance travelled by spore (h_r = 2 m)

B) Distance travelled by spore (h_r = 5 m)

C) Distance travelled by spore (h_r = 10 m)

Figure 5. Model outputs of probability density functions for distance travelled by spores in a forested environment. Panels A, B, and C had different spore release heights (hr) inputted into the model- 2, 5, and 10 m respectively. Solid lines are in different colours for each of the low (black), low-medium(blue), medium-high(yellow) and high (red) U_{h_c} (wind speed) cases. Dashed lines show modal D
330 **(distance) travelled by the spores. n = 1,000,000 for each case.**
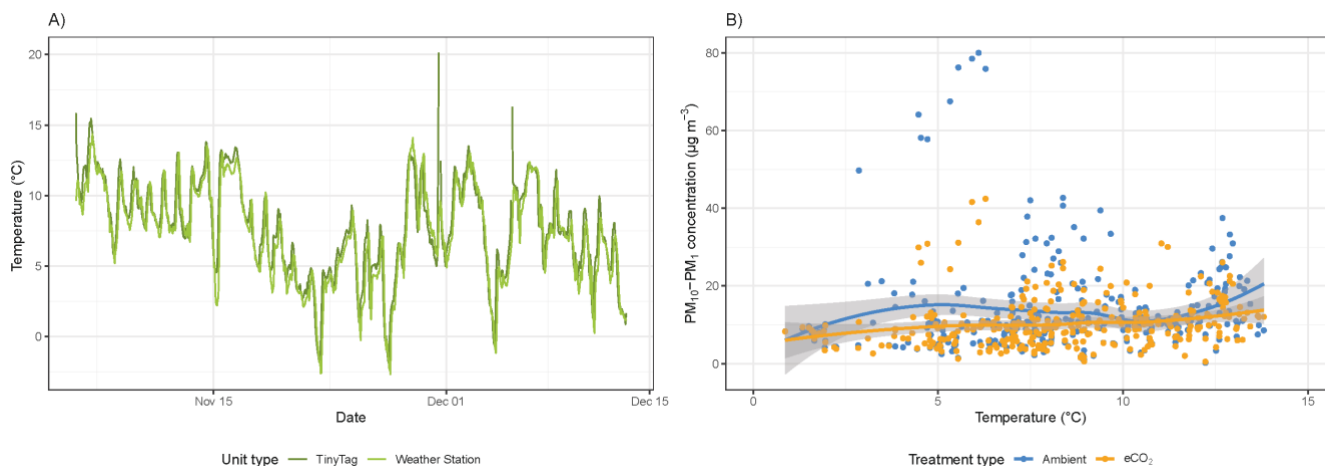
Figure 6. Temperature and bioaerosol (PM_{10}-PM_1) concentrations across the experimental duration at BIFoR FACE. Panel A shows temperature data, with mean temperature measured by TinyTag sensors shown in dark green, and light green showing data collected by the Array 1 weather station. Panel B compares temperature data with bioaerosol concentrations, with data from ambient arrays
335 **(Arrays 2,3,and 5) in blue, and data from eCO₂ arrays (Arrays 1,4, and 6) in orange, with both treatment types fitted with a loess line (Wickham et al., 2019).**

3.2 Hypothesis B: Fungal bioaerosol concentrations will increase in woodland patches treated with eCO₂ for two years.

Figure 7 shows six plots comparing PM_{10}-PM_1 concentrations between the eCO₂ (orange) and ambient (blue) arrays. When comparing total concentrations across the entire measurement period (Figure 7 Panels A, B, and C), there was no significant
340 difference (p = 0.489) between the eCO₂ treatment and ambient, however a heavy tail is present in the ambient arrays. To investigate this relationship further, we separated out the data into low bioaerosol concentration conditions ($<10\ \mu g\ m^{-3}$) and high bioaerosol concentrations ($>= 10 \mu g\ m^{-3}$) (Figure 7 Panels D, E, and F). When bioaerosol concentration are low (Figure 7**Error! Reference source not found.** Panels D and E), there was no significant difference between the eCO₂ and ambient treatments (p = 0.689). These low concentrations likely represent background levels of aerosols that are consistent throughout
345 the forest. However, when selecting for high concentration events, there was a significant effect seen, whereby eCO₂ treatment suppressed concentrations of high bioaerosol events (p = 0.023) (Figure 7 Panels D and F).

The boxplot in Panel A shows that there is no significant difference between the medians of eCO₂ treatment versus the control; however, there were slightly higher bioaerosol concentrations shown under ambient conditions. Panel B shows a time series
350 of the data, demonstrating that bioaerosol concentrations match extremely closely between the two treatment groups. The small difference in the overall medians can be largely attributed to the PM_{10}-PM_1 concentration difference between the eCO₂ and

15

ambient during the largest bioaerosol event around the 22nd of November (during the second measurement period, shown shaded in grey), where the ambient array (shown in blue) measures higher than the eCO$_2$ array in orange.
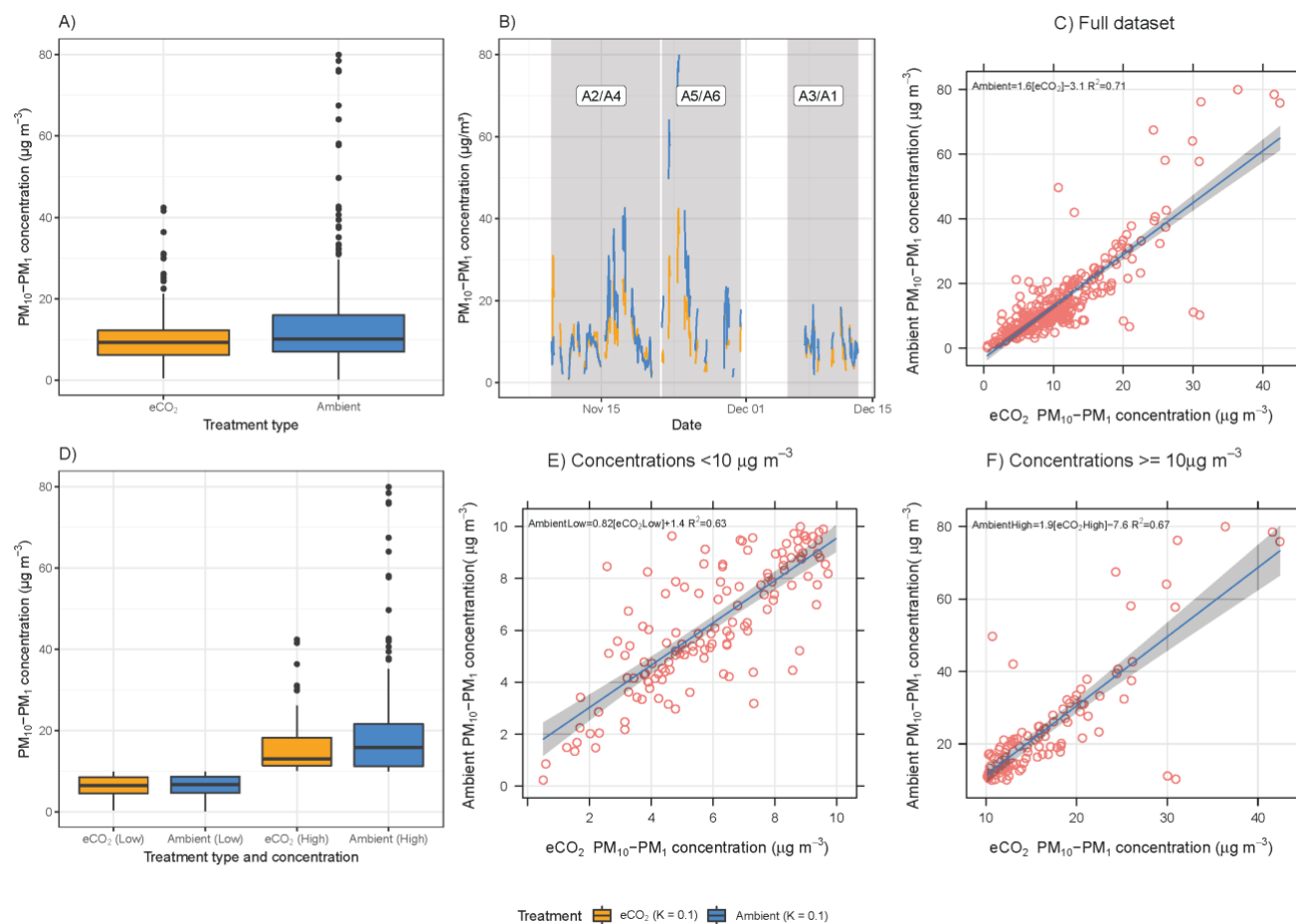
Figure 7. Bioaerosol concentrations across the experimental duration in ambient (Arrays 2,3, and 5) and eCO$_2$ (Arrays 1, 4, and 6) arrays. eCO$_2$ treatment is shown in orange, ambient control in blue. Panels A, B, and C include the full dataset, with no significant difference shown between the eCO2 treatment and control. Panels D, E, and F split the dataset into low (<10 μg m^{-3}) and high (>=10 μg m^{-3}) bioaerosol concentrations. When the data is split in this way, there was no significant difference between treatments under low bioaerosol concentrations. However, when bioaerosol concentrations were high, concentrations were significantly lower under eCO$_2$ treatment.

4. Discussion

In support of hypothesis A, we found that various meteorological variables affected bioaerosol concentrations. The RH before correction was of particular importance, especially as the low-cost OPCs do not have any warming or drying capacity, and therefore are susceptible to recording higher mass concentrations of aerosols under high humidity conditions as particles swell with additional water (Crilley et al., 2018). We found that the RH % threshold for significant particle swelling was 90–95%,

which is a much higher RH value than would be expected for anthropogenic aerosols, which typically contain more hygroscopic components including salts, and therefore provides evidence that the measured PM_{10}–PM_1 fraction represents a predominantly biological source. In their study investigating effects of RH on fungal spore swelling, Reponen et al. (1996) demonstrated a similar effect whereby a significant swelling of fungal spores was seen, but only at very high humidities (greater

370 than 90%). We believe this threshold for particle swelling further demonstrates that we are recording a biological source. This hygroscopic evidence is in addition to the ecological and phenological evidence for spores being the dominant source within the PM_{10}-PM_1 size fraction during the measurement period.

After correction, we did not see any effect of RH on fungal spore concentrations. The evidence in the literature for the relationship between spore concentrations and RH is mixed, probably largely due to species-specific effect. Some fungal

375 species are dependent on high RH to develop spores (and then release spores by rain droplets), whereas other species release spores in response to a drop in RH (Jones and Harrison, 2004; Li and Kendrick, 1995). The high diversity of fungal species at BIFoR (each with possibly varying responses to RH) could result in this flat line. Another possible explanation is that the fungi never experience low RH conditions due to the constant high RH at BIFoR FACE, potentially with the RH never dropping low enough to trigger a burst of spore release. Finally, it is important to mention that although the Crilley correction is an

380 essential part of using low-cost sensors in a high-humidity environment, the high swelling threshold of fungal spores means that the κ value of 0.3 (or even 0.1) may be inappropriately high for biological particles such as these. As shown in Figure 2 Panel B and C, after correcting the data, the PM_{10}–PM_1 concentrations decrease after 95% RH, although this effect is smaller when using a κ of 0.1. For future studies, calibrating the low-cost OPCs against a reference grade instrument in the experimental environment in order to provide a calibrated κ-value would be an appropriate measure, and enable a more thorough

385 investigation of the RH dependence, and improve the accuracy of the Crilley correction for bioaerosols (Crilley et al., 2020). We measured an approximately U-shaped curve of bioaerosol concentrations in response to wind speed, with the highest PM_{10}–PM_1 concentrations being displayed at low and high wind speeds. This likely indicates a balance between spore release mechanisms and mixing of low-aerosol air. At low wind speeds, there is minimal movement of air through the forest, so any spores released do not travel significant distances. At high wind speeds, there is much higher movement of air, which decreases

390 concentrations by carrying spores further; however, spore release by wind could also be increased (Dressaire et al., 2016). At medium wind speeds, a balance between these two effects occurs, maintaining bioaerosol concentrations at a lower level (Jones and Harrison, 2004).

Our model demonstrated that under low wind-speed conditions, spores are most likely to travel a relatively short distance, suggesting that between-array mixing was unlikely under the meteorological conditions experienced during the measurement

395 period. Particle release height (h_r) had a significant impact on the distance travelled by a particle, which is an important consideration given the source of bioaerosols. For example, fungal spores are likely to have a significantly lower h_r than pollen which, based on our model, would significantly impact the distance travelled by the different bioaerosol types. Due to the complexity of the forest environment, there are a number of aspects which the model did not capture which could alter the distance travelled by a spore. Complex wind dynamics such as ejections (infrequent but strong upward gusts of air) and

400   turbulence around forest edges could increase the distance travelled by a spore, as well as varied spore release dynamics between fungi (Dressaire et al., 2016; Norros et al., 2014). The model also assumes a spatially representative wind speed profile, which does not account for local velocity effects induced by gaps, clearings, and changes in canopy density. These local effects may be important near the ground, where wind speeds are generally low. However, the distance travelled could also be shorter than modelled, for example, the model does not capture spore deposition onto forest surfaces other than the

405   ground, spores being swept downwards by gusts, and changes with wet versus dry deposition.

The data demonstrated a decrease in bioaerosol concentrations at lower temperatures, which is the expected response within the range of temperatures we observed in a woodland of this type (Gange et al., 2007). The number of fungal sporocarps present across the duration of the experiment decreased, and it is therefore logical to expect that spore production would also consequently decrease. For future studies, it would be interesting to begin measurements earlier in the fungal season, allowing

410   us to capture the peak of sporocarp production, as well as the end of the active eCO_2 fumigation at the FACE experiment.

Regarding Hypothesis B, to our knowledge, this is the first assessment of bioaerosols in any forest FACE experiment to date, and therefore provides valuable data contributing to the understanding of the forest environment at BIFoR FACE as well as more broadly in the context of forests, and FACE experiments. We did not see a significant effect of eCO_2 on total aerosol concentrations. However, when data was split into low and high aerosol concentrations, two differing responses were

415   demonstrated. Under low concentrations, there was no significant effect of eCO_2 treatment, we therefore think these low concentrations represent the background concentrations of aerosols present both inside and in the wider environment around the forest. However, when high concentrations of bioaerosols were detected, eCO_2 treatment resulted in a suppression of PM_{10}-PM_1 concentrations. This is demonstrated in a number of larger sporulation events during the experimental period, for example the large sporulation event peaking on 22nd November, where although both arrays showed the sporulation event, the magnitude

420   of this event was significantly different between eCO_2 and ambient.

This evidence, as well as the eCO_2 dispersal data from Hart et al., 2019, and the modal spore travel distances shown in our model suggests to us that this experimental set-up is capable of detecting differences between the eCO_2 and ambient arrays. It is apparent that at background concentrations these differences are not present between arrays, however there may be a

425   response to eCO_2 during large sporulation events. This could be for a number of reasons, the primary reason being that the experiment was in the very early stages of fumigation (year two of ten total years planned), and there might be a lag expected in fungal responses, as they are most likely responding indirectly to eCO_2 via changes in leaf litter and soil. Although the literature states a small number of cases of where individual fungal species do respond directly to eCO_2, it is likely that the main effects would be secondary, for example, competition between autotrophs and heterotrophs for nutrients, or an increase

430   in leaf litter production resulting in an increase the population of decomposer fungi. There is evidence for increased autotrophic productivity under eCO_2 at BIFoR FACE in the form of increased leaf-scale photosynthesis (Gardner et al., 2020) and fine root production (Ziegler et al., 2021). Whether this increased autotrophic productivity primes, or competes with, fungal activity requires further work. Continuing to monitor bioaerosol concentrations throughout the 10+ year experimental duration of the

BIFoR FACE experiment, along with monitoring in other FACE experiments, will be key in understanding how eCO$_2$ affects

435 bioaerosol concentrations long term.

Another possible reason for not picking up an eCO$_2$ response in fungal bioaerosols in the full dataset is that the maximum diameter of the particles that can be detected by the OPCs is 10 µm, which does exclude several fungal species, including those known to be present in the BIFoR forest during the experimental duration. If a response to eCO$_2$ is species-specific, then it is possible that we are missing an effect in fungi with larger spores. It is also possible that although the total and background

440 aerosol concentration was stable under eCO$_2$, the aerosol composition could have been different (e.g. altered ratios of fungal species present), which we were not able to detect using the OPCs. Varying fungal species between the ambient and eCO$_2$ arrays could therefore be responsible for the differing response we detected during sporulation events. In order to determine definitive particle composition, other techniques such as detectors using fluorescence, or DNA sequencing of biological material is required (Fröhlich-Nowoisky et al., 2016; Gosselin et al., 2016; Healy et al., 2012). Finally, our experimental

445 measurement period occurred outside of the eCO$_2$ fumigation season, and therefore the main growing season of the trees, which could have reduced any direct effects of the eCO$_2$, although, given the likely cumulative effect of the eCO$_2$ treatment over the growing season, and the fact that our measurements were focused on the period of peak sporulation, it seems more likely that our measurements were well-timed to observe any treatment effects.

5 Conclusions

450 We have demonstrated that low-cost OPCs are suitable for measuring bioaerosol concentrations in forests, or other high-humidity environments. This has consequences for other research into the aerobiology of forests, and also opens up the bioaerosol research field to a wider array of locations and researchers. The low-cost sensors measured significant swelling in PM$_{10}$–PM$_1$ sized particles at very high RH, which we corrected for using a calibration factor from Crilley et al. (2018). For future work, generating a κ value using a reference-grade instrument in situ would improve accuracy (Crilley et al., 2020).

455 Temperature, wind speed, and wind direction were all shown to affect bioaerosol concentrations; however, we did not see any effect of RH (post-correction). Treatment with eCO2 may repress concentrations of bioaerosols during high sporulation events, however this significant difference was not detected across all concentrations of aerosols. Therefore, further investigation later in the 10+ year experimental duration is warranted, as well as investigating forest bioaerosols in other forest FACE experiments globally.

6 Data availability

460

Data supporting this publication are openly available from the UBIRA eData repository at https://doi.org/10.25500/edata.bham.00000688. The data provided is the hourly data with the inter-unit calibration bias factor applied.

7 Author contribution

ABB and FDP designed the bioaerosol study as part of the FACE programme designed by ARMK. ABB collected and analysed the OPC data and prepared the manuscript. EJB wrote the model. All co-authors discussed the results and contributed to writing the manuscript.

8 Competing interests

The authors declare that they have no conflicts of interest.

9 Acknowledgements

10 References

Amiro, B.D., 1990. Comparison of turbulence statistics within three boreal forest canopies. Boundary-Layer Meteorology 51, 99–121. https://doi.org/10.1007/BF00120463

Andrew, C., Lilleskov, E.A., 2009. Productivity and community structure of ectomycorrhizal fungal sporocarps under increased atmospheric CO2 and O3. Ecology Letters 12, 813–822. https://doi.org/10.1111/j.1461-0248.2009.01334.x

Aylor, D.E., 1978. Dispersal in Time and Space: Aerial Pathogens, in: Horsfall, J.G., Cowling, E.B. (Eds.), Plant Disease: An Advanced Treatise. Academic Press, New York, pp. 159–179. https://doi.org/10.1016/0048-3575(79)90101-9

Baird, A.B., Pope, F.D., 2021. "Can't see the forest for the trees": The importance of fungi in the context of UK tree planting. Food and Energy Security (In review).

Baldocchi, D.D., Meyers, T.P., 1988. Turbulence structure in a deciduous forest. Boundary-Layer Meteorology 43, 345–364.

Bannister, E., MacKenzie, A.R., Cai, X., 2021. Realistic forests and the modeling of forest-atmosphere exchange [WWW Document]. Earth and Space Science Open Archive. https://doi.org/10.1002/essoar.10506854.1

Belcher, S.E., Harman, I.N., Finnigan, J.J., 2012. The Wind in the Willows: Flows in Forest Canopies in Complex Terrain. Annual Review of Fluid Mechanics 44, 479–504. https://doi.org/10.1146/annurev-fluid-120710-101036

Biedermann, P.H.W., Vega, F.E., 2020. Ecology and Evolution of Insect–Fungus Mutualisms. Annual Review of Entomology 65, 431–455. https://doi.org/10.1146/annurev-ento-011019-024910

495 Burge, H.A., 2002. An update on pollen and fungal spore aerobiology. Journal of Allergy and Clinical Immunology 110, 544–552. https://doi.org/10.1067/mai.2002.128674

Carslaw, D.C., Ropkins, K., 2012. openair --- an R package for air quality data analysis. Environmental Modelling & Software. 27–28, 52–61.

Chaudhary, V.B., Nolimal, S., Sosa-Hernández, M.A., Egan, C., Kastens, J., 2020. Trait-based aerial dispersal of arbuscular
500 mycorrhizal fungi. New Phytologist n/a. https://doi.org/10.1111/nph.16667

Cionco, R.M., 1978. Analysis of canopy index values for various canopy densities. Boundary-Layer Meteorology 15, 81–93. https://doi.org/10.1007/BF00165507

Cionco, R.M., 1965. A Mathematical Model for Air Flow in a Vegetative Canopy. Journal of Applied Meteorology. https://doi.org/10.1175/1520-0450(1965)004<0517:ammfaf>2.0.co;2

505 Crilley, L.R., Shaw, M., Pound, R., Kramer, L.J., Price, R., Young, S., Lewis, A.C., Pope, F.D., 2018. Evaluation of a low-cost optical particle counter (Alphasense OPC-N2) for ambient air monitoring. Atmos. Meas. Tech 11, 709–720. https://doi.org/10.5194/amt-11-709-2018

Crilley, L.R., Singh, A., Kramer, L.J., Shaw, M.D., Alam, M.S., Apte, J.S., Bloss, W.J., Hildebrandt Ruiz, L., Fu, P., Fu, W., Gani, S., Gatari, M., Ilyinskaya, E., Lewis, A.C., Ng'ang'a, D., Sun, Y., Whitty, R.C.W., Yue, S., Young, S., Pope, F.D., 2020.
510 Effect of aerosol composition on the performance of low-cost optical particle counter correction factors. Atmospheric Measurement Techniques 13, 1181–1193. https://doi.org/10.5194/amt-13-1181-2020

Davies, R.R., Denny, M.J., Newton, L.M., 1963. A Comparison Hetween the Summer and Autumn Air-Sporas at London and Liverpool. Allergy 18, 131–147. https://doi.org/10.1111/j.1398-9995.1963.tb03156.x

Di-Giovanni, F., Kevan, P.G., Nasr, M.E., 1995. The variability in settling velocities of some pollen and spores. Grana 34, 39–
515 44. https://doi.org/10.1080/00173139509429031

Dressaire, E., Yamada, L., Song, B., Roper, M., 2016. Mushrooms use convectively created airflows to disperse their spores. Proc Natl Acad Sci U S A 113, 2833–2838. https://doi.org/10.1073/pnas.1509612113

Finnigan, J., 2000. Turbulence in Plant Canopies. Annual Review of Fluid Mechanics 32, 519–571.

Fröhlich-Nowoisky, J., Kampf, C.J., Weber, B., Huffman, J.A., Pöhlker, C., Andreae, M.O., Lang-Yona, N., Burrows, S.M.,
520 Gunthe, S.S., Elbert, W., Su, H., Hoor, P., Thines, E., Hoffmann, T., Després, V.R., Pöschl, U., 2016. Bioaerosols in the Earth system: Climate, health, and ecosystem interactions. Atmospheric Research 182, 346–376. https://doi.org/10.1016/j.atmosres.2016.07.018

Fröhlich-Nowoisky, J., Pickersgill, D.A., Despres, V.R., Poschl, U., 2009. High diversity of fungi in air particulate matter. Proceedings of the National Academy of Sciences 106, 12814–12819. https://doi.org/10.1073/pnas.0811003106

525   Gange, A.C., Gange, E.G., Sparks, T.H., Boddy, L., 2007. Rapid and Recent Changes in Fungal Fruiting Patterns. Science 316, 71–71. https://doi.org/10.1126/science.1137489

Gardner, A., Ellsworth, D.S., Crous, K.Y., Pritchard, J., MacKenzie, A.R., 2020. Is photosynthetic enhancement sustained through three years of elevated CO2 exposure in 175-year old Quercus robur? bioRxiv 2020.12.16.416255. https://doi.org/10.1101/2020.12.16.416255

530   Gilbert, G.S., Reynolds, D.R., 2005. Nocturnal Fungi: Airborne Spores in the Canopy and Understory of a Tropical Rain Forest. Biotropica 37, 462–464.

Gosselin, M.I., Rathnayake, C.M., Crawford, I., Pöhlker, C., Fröhlich-Nowoisky, J., Schmer, B., Després, V.R., Engling, G., Gallagher, M., Stone, E., Pöschl, U., Huffman, J.A., 2016. Fluorescent bioaerosol particle, molecular tracer, and fungal spore concentrations during dry and rainy periods in a semi-arid forest. Atmos. Chem. Phys. 16, 15165–15184.

535   https://doi.org/10.5194/acp-16-15165-2016

Griffiths, P.T., Borlace, J.-S., Gallimore, P.J., Kalberer, M., Herzog, M., Pope, F.D., 2012. Hygroscopic growth and cloud activation of pollen: a laboratory and modelling study. Atmospheric Science Letters 13, 289–295. https://doi.org/10.1002/asl.397

Grinn-Gofroń, A., Nowosad, J., Bosiacka, B., Camacho, I., Pashley, C., Belmonte, J., De Linares, C., Ianovici, N., Manzano,

540   J.M.M., Sadyś, M., Skjøth, C., Rodinkova, V., Tormo-Molina, R., Vokou, D., Fernández-Rodríguez, S., Damialis, A., 2019. Airborne Alternaria and Cladosporium fungal spores in Europe: Forecasting possibilities and relationships with meteorological parameters. Science of The Total Environment 653, 938–946. https://doi.org/10.1016/j.scitotenv.2018.10.419

Grundström, M., Adams-Groom, B., Pashley, C.H., Dahl, Å., Rasmussen, K., de Weger, L.A., Thibaudon, M., Fernández-Rodríguez, S., Silva-Palacios, I., Skjøth, C.A., 2019. Oak pollen seasonality and severity across Europe and modelling the

545   season start using a generalized phenological model. Science of The Total Environment 663, 527–536. https://doi.org/10.1016/j.scitotenv.2019.01.212

Hagan, D., 2017. py-opc, available at https://github.com/dhhagan/py-opc [WWW Document]. URL https://github.com/dhhagan/py-opc (accessed 1.27.21).

Halbwachs, H., Bässler, C., 2015. Gone with the wind – a review on basidiospores of lamellate agarics. Mycosphere 6, 78–

550   112. https://doi.org/10.5943/mycosphere/6/1/10

Hart, K.M., Curioni, G., Blaen, P., Harper, N.J., Miles, P., Lewin, K.F., Nagy, J., Bannister, E.J., Cai, X.M., Thomas, R.M., Krause, S., Tausz, M., MacKenzie, A.R., 2019. Characteristics of Free Air Carbon Dioxide Enrichment of a Northern Temperate Mature Forest. Global Change Biology 0. https://doi.org/10.1111/gcb.14786

Heald, C.L., Spracklen, D.V., 2009. Atmospheric budget of primary biological aerosol particles from fungal spores.

555   Geophysical Research Letters 36. https://doi.org/10.1029/2009GL037493

Healy, D.A., O'Connor, D.J., Sodeau, J.R., 2012. Measurement of the particle counting efficiency of the "Waveband Integrated Bioaerosol Sensor" model number 4 (WIBS-4). Journal of Aerosol Science 47, 94–99. https://doi.org/10.1016/j.jaerosci.2012.01.003

Hollins, P.D., Kettlewell, P.S., Atkinson, M.D., Stephenson, D.B., Corden, J.M., Millington, W.M., Mullins, J., 2004.
560   Relationships between airborne fungal spore concentration of Cladosporium and the summer climate at two sites in Britain.
Int J Biometeorol 48, 137–141. https://doi.org/10.1007/s00484-003-0188-9

Horton, T.R., 2017. Spore Dispersal in Ectomycorrhizal Fungi at Fine and Regional Scales, in: Tedersoo, L. (Ed.),
Biogeography of Mycorrhizal Symbiosis, Ecological Studies. Springer International Publishing, Cham, pp. 61–78.
https://doi.org/10.1007/978-3-319-56363-3_3

565   Jones, A.M., Harrison, R.M., 2004. The effects of meteorological factors on atmospheric bioaerosol concentrations—a review.
Science of The Total Environment 326, 151–180. https://doi.org/10.1016/j.scitotenv.2003.11.021

Kaimal, J.C., Finnigan, J.J., 1994. Atmospheric boundary layer flows—their structure and measurement. Oxford University
Press, New York. https://doi.org/10.16085/j.issn.1000-6613.2012.02.016

Kauserud, H., Heegaard, E., Buntgen, U., Halvorsen, R., Egli, S., Senn-Irlet, B., Krisai-Greilhuber, I., Damon, W., Sparks, T.,
570   Norden, J., Hoiland, K., Kirk, P., Semenov, M., Boddy, L., Stenseth, N.C., 2012. Warming-induced shift in European
mushroom fruiting phenology. Proceedings of the National Academy of Sciences 109, 14488–14493.
https://doi.org/10.1073/pnas.1200789109

Kivlin, S.N., Winston, G.C., Goulden, M.L., Treseder, K.K., 2014. Environmental filtering affects soil fungal community
composition more than dispersal limitation at regional scales. Fungal Ecology, Fungal ecology beyond boundaries: from
575   communities to the globe 12, 14–25. https://doi.org/10.1016/j.funeco.2014.04.004

Klironomos, J.N., Rillig, M.C., Allen, M.F., Zak, D.R., Pregitzer, K.S., Kubiske, M.E., 1997. Increased levels of airborne
fungal spores in response to *Populus tremuloides* grown under elevated atmospheric CO_2. Can. J. Bot. 75, 1670–1673.
https://doi.org/10.1139/b97-880

Læssøe, T., Petersen, J.H., 2019. Fungi of Temperate Europe. Princeton University Press.

580   Li, D.-W., Kendrick, B., 1995. A year-round study on functional relationships of airborne fungi with meteorological factors.
Int J Biometeorol 39, 74–80. https://doi.org/10.1007/BF01212584

Lilleskov, E.A., Bruns, T.D., 2005. Spore dispersal of a resupinate ectomycorrhizal fungus, Tomentella sublilacina, via soil
food webs. Mycologia 97, 762–769. https://doi.org/10.1080/15572536.2006.11832767

MacKenzie, A.R., Krause, S., Hart, K., Thomas, R., Blaen, P., Hamilton, R., Curioni, G., Quick, S., Kourmouli, A., Hannah,
585   D., Warner, S.C., Brekenfeld, N., Ullah, S., Press, M., 2020. BIFoR FACE: Water-soil-vegetation-atmosphere research in a
temperate   deciduous   forest   catchment,   including   under   elevated   CO2   (preprint).   Preprints.
https://doi.org/10.22541/au.160157598.86879557

Moore-Landecker,   E.,   2011.   Fungal   Spores,   in: ELS.   American   Cancer   Society.
https://doi.org/10.1002/9780470015902.a0000378.pub2

590   Nathan, R., Horn, H.S., Chave, J., Levin, S.A., 2002. Mechanistic models for tree seed dispersal by wind in dense forests and
open landscapes., in: Levey, D.J., Silva, W.R., Galetti, M. (Eds.), Seed Dispersal and Frugivory: Ecology, Evolution and

Conservation. Third International Symposium-Workshop on Frugivores and Seed Dispersal, São Pedro, Brazil, 6-11 August 2000. CABI, Wallingford, pp. 69–82. https://doi.org/10.1079/9780851995250.0069

National Pollen and Aerobiology Research Unit, 2012. . Pollen Calendars by area - University Of Worcester. URL

595   https://www.worcester.ac.uk/about/academic-schools/school-of-science-and-the-environment/science-and-the-environment-research/national-pollen-and-aerobiology-research-unit/pollen-calendar.aspx (accessed 7.16.20).

Norby, R.J., De Kauwe, M.G., Domingues, T.F., Duursma, R.A., Ellsworth, D.S., Goll, D.S., Lapola, D.M., Luus, K.A., MacKenzie, A.R., Medlyn, B.E., Pavlick, R., Rammig, A., Smith, B., Thomas, R., Thonicke, K., Walker, A.P., Yang, X., Zaehle, S., 2016. Model-data synthesis for the next generation of forest free-air CO_2 enrichment (FACE) experiments. New

600   Phytologist 209, 17–28. https://doi.org/10.1111/nph.13593

Norros, V., Penttilä, R., Suominen, M., Ovaskainen, O., 2012. Dispersal may limit the occurrence of specialist wood decay fungi already at small spatial scales. Oikos 121, 961–974. https://doi.org/10.1111/j.1600-0706.2012.20052.x

Norros, V., Rannik, Ü., Hussein, T., Petäjä, T., Vesala, T., Ovaskainen, O., 2014. Do small spores disperse further than large spores? Ecology 95, 1612–1621. https://doi.org/10.1890/13-0877.1

605   O'Connor, D.J., Sadyś, M., Skjøth, C.A., Healy, D.A., Kennedy, R., Sodeau, J.R., 2014. Atmospheric concentrations of Alternaria, Cladosporium, Ganoderma and Didymella spores monitored in Cork (Ireland) and Worcester (England) during the summer of 2010. Aerobiologia 30, 397–411. https://doi.org/10.1007/s10453-014-9337-3

Oneto, D.L., Golan, J., Mazzino, A., Pringle, A., Seminara, A., 2020. Timing of fungal spore release dictates survival during atmospheric transport. PNAS 117, 5134–5143. https://doi.org/10.1073/pnas.1913752117

610   Page, C.N., 1997. The Ferns of Britain and Ireland, 2nd ed. CUP.

Petters, M.D., Kreidenweis, S.M., 2007. A single parameter representation of hygroscopic growth and cloud condensation nucleus activity. Atmospheric Chemistry and Physics 7, 1961–1971. https://doi.org/10.5194/acp-7-1961-2007

Pope, F.D., 2010. Pollen grains are efficient cloud condensation nuclei. Environ. Res. Lett. 5, 044015. https://doi.org/10.1088/1748-9326/5/4/044015

615   Pöschl, U., 2005. Atmospheric Aerosols: Composition, Transformation, Climate and Health Effects. Angewandte Chemie International Edition 44, 7520–7540. https://doi.org/10.1002/anie.200501122

Raupach, M.R., Finnigan, J.J., Brunet, Y., 1996. Coherent Eddies and Turbulence in Vegetation Canopies: The Mixing-Layer Analogy. Boundary-Layer Meteorology 25th Anniversary Volume, 1970–1995 351–382. https://doi.org/10.1007/978-94-017-0944-6_15

620   Reinmuth-Selzle, K., Kampf, C.J., Lucas, K., Lang-Yona, N., Fröhlich-Nowoisky, J., Shiraiwa, M., Lakey, P.S.J., Lai, S., Liu, F., Kunert, A.T., Ziegler, K., Shen, F., Sgarbanti, R., Weber, B., Bellinghausen, I., Saloga, J., Weller, M.G., Duschl, A., Schuppan, D., Pöschl, U., 2017. Air Pollution and Climate Change Effects on Allergies in the Anthropocene: Abundance, Interaction, and Modification of Allergens and Adjuvants. Environ Sci Technol 51, 4119–4141. https://doi.org/10.1021/acs.est.6b04908

625 Reponen, T., Willeke, K., Ulevicius, V., Reponen, A., Grinshpun, S.A., 1996. Effect of relative humidity on the aerodynamic diameter and respiratory deposition of fungal spores. Atmospheric Environment 30, 3967–3974. https://doi.org/10.1016/1352-2310(96)00128-8

Sadyś, M., Adams-Groom, B., Herbert, R.J., Kennedy, R., 2016a. Comparisons of fungal spore distributions using air sampling at Worcester, England (2006–2010). Aerobiologia 32, 619–634. https://doi.org/10.1007/s10453-016-9436-4

630 Sadyś, M., Kennedy, R., West, J.S., 2016b. Potential impact of climate change on fungal distributions: analysis of 2 years of contrasting weather in the UK. Aerobiologia 32, 127–137. https://doi.org/10.1007/s10453-015-9402-6

Sadyś, M., Skjøth, C.A., Kennedy, R., 2014. Back-trajectories show export of airborne fungal spores (Ganoderma sp.) from forests to agricultural and urban areas in England. Atmospheric Environment 84, 88–99. https://doi.org/10.1016/j.atmosenv.2013.11.015

635 Sesartic, A., Dallafior, T.N., 2011. Global fungal spore emissions, review and synthesis of literature data. Biogeosciences 8, 1181–1192. https://doi.org/10.5194/bg-8-1181-2011

Sousan, S., Koehler, K., Hallett, L., Peters, T.M., 2016. Evaluation of the Alphasense optical particle counter (OPC-N2) and the Grimm portable aerosol spectrometer (PAS-1.108). Aerosol Science and Technology 50, 1352–1365. https://doi.org/10.1080/02786826.2016.1232859

640 Stephens, R.B., Rowe, R.J., 2020. The underappreciated role of rodent generalists in fungal spore dispersal networks. Ecology 101, e02972. https://doi.org/10.1002/ecy.2972

Su, H.B., Shaw, R.H., Pawu, K.T., Moeng, C.H., Sullivan, P.P., 1998. Turbulent statistics of neutrally stratified flow within and above a sparse forest from large-eddy simulation and field observations. Boundary-Layer Meteorology 88, 363–397. https://doi.org/10.1023/A:1001108411184

645 Tesmer, J., Schnittler, M., 2007. Sedimentation velocity of myxomycete spores. Mycological Progress 6, 229–234. https://doi.org/10.1007/s11557-007-0539-8

Wickham, H., Averick, M., Bryan, J., Chang, W., McGowan, L.D., François, R., Grolemund, G., Hayes, A., Henry, L., Hester, J., Kuhn, M., Pedersen, T.L., Miller, E., Bache, S.M., Müller, K., Ooms, J., Robinson, D., Seidel, D.P., Spinu, V., Takahashi, K., Vaughan, D., Wilke, C., Woo, K., Yutani, H., 2019. Welcome to the Tidyverse. Journal of Open Source Software 4, 1686.

650 https://doi.org/10.21105/joss.01686

Wolf, J., Johnson, N.C., Rowland, D.L., Reich, P.B., 2003. Elevated CO2 and plant species richness impact arbuscular mycorrhizal fungal spore communities. New Phytologist 157, 579–588.

Wolf, J., O'Neill, N.R., Rogers, C.A., Muilenberg, M.L., Ziska, L.H., 2010. Elevated atmospheric carbon dioxide concentrations amplify Alternaria alternate sporulation and total antigen production. Environmental Health Perspectives 118,

655 1223–1228. https://doi.org/10.1289/ehp.0901867

Ziegler, C., Kulawska, A., Kourmouli, A., Hamilton, L., Shi, Z., MacKenzie, A.R., Dyson, R.J., Johnston, I.G., 2021. Quantification and uncertainty of root growth stimulation by elevated CO2 in mature temperate deciduous forest. bioRxiv 2021.04.15.440027. https://doi.org/10.1101/2021.04.15.440027